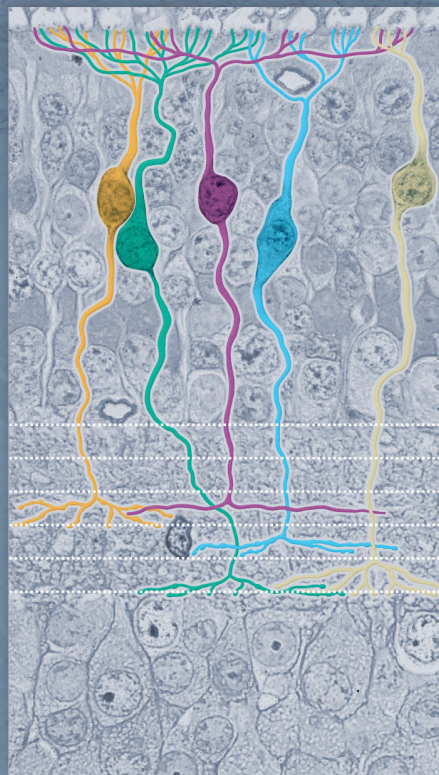
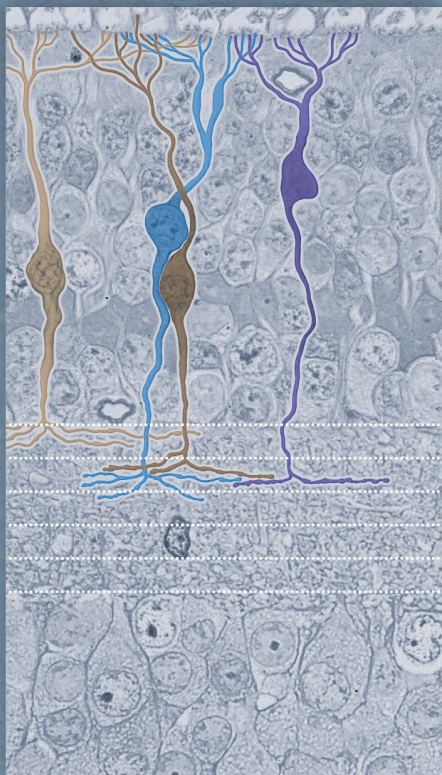
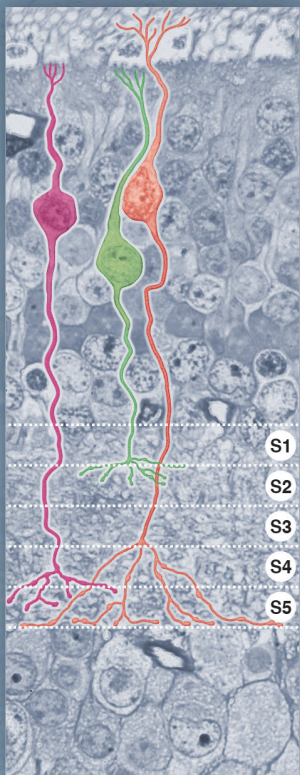
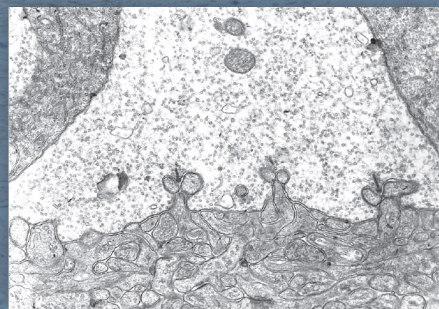
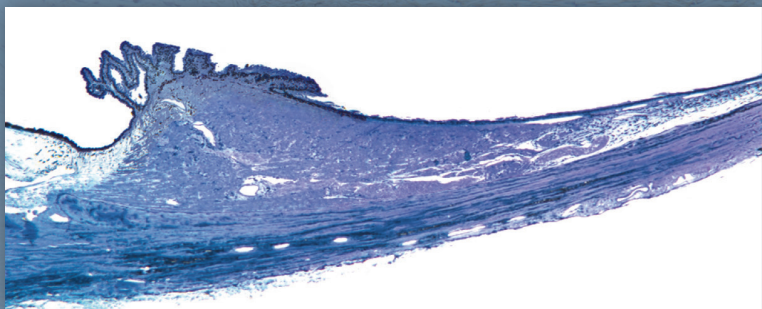


EUGENIO BERTELLI

Anatomy of the Eye and Human Visual System



PICCIN

CHAPTER 1

Orbit

Eugenio Bertelli

List of Abbreviations

IOF	Inferior Orbital Fissure
IR	Inferior Rectus
LP	Levator Palpebrae superioris
LR	Lateral Rectus
MR	Medial Rectus muscle
SOF	Superior Orbital Fissure

General Features

Human orbits are a pair of symmetric cavities lying beside the root of the nose (Fig. 1.1). The two orbits are separated from each other by the nasal cavities and the ethmoidal sinuses. They lie over the maxillary sinuses, below the anterior cranial fossa, and are medial to the temporal and middle cranial fossae. Each orbit has the shape of a quadrangular pyramid lying horizontally, with the base facing forward, laterally and slightly downward, and the apex directed backward and medially. The base of the orbit is known as the **anterior orbital opening** and the apex corresponds to the **optic foramen**. Orbit comparison with a pyramid, frequently used for descriptive purposes, falls short for two main reasons. Firstly, as the floor is shorter than the other walls, frontal sections show a quadrilateral profile only in the anterior orbit whereas more posterior sections assume a triangular shape (Fig. 1.2); secondly, the maximum diameter of the orbit is not at its base but about 1 cm behind it. For these reasons, the shape of the orbit could be also compared to a pear with the stalk in the optic canal. Nevertheless, we will stick to the quadrangular pyramid as the shape of reference, describing one by one its constitutive elements: the four walls (superior, inferior, lateral and medial), the four angles, the apex and the base with its margins.

The medial wall of the orbit lies along a sagittal plane whereas the lateral wall diverges from the former by a 45° angle. Variations of this angle are common and are related to the individual variability of the head conformation. The longitudinal axis of the orbit, 44 to 50 mm long, is oriented forward, laterally and downward and makes a 22-23° angle with the sagittal plane (Fig. 1.3).

The size of the orbit, particularly with regard to its depth, greatly varies according to individuals, sex, race and age. Its average volume is about 30 mL, while the average volume of the eyeball is 7.5 mL. Overall, human orbit is outlined by seven bones: frontal, ethmoid, sphenoid, lacrimal, maxillary, zygomatic and palatine bones (Fig. 1.4). The orbit walls are traversed by several canals/openings through which vessels and nerves enter and leave the orbital cavity (Table 1.1, see p. 17).

Inferolateral Angle

The posterior half of the inferolateral angle is occupied by the **inferior orbital fissure (IOF)** (Fig. 1.12), a 20 mm elongated opening bounded medially by the maxilla and the orbital process of the palatine bone, and laterally by the inferior margin of the orbital surface of the greater wing of the sphenoid; the zygomatic bone completes the fissure anteriorly in about 60% of cases. Through the IOF the orbit joins the infraorbital fossa and, at the posterior end of the fissure, the pterygopalatine fossa. As the posterior extremity of the IOF is also located just under the posterior part of the superior orbital fissure (SOF), it roughly represents the converging point of the openings connecting the orbit with three important and very different anatomic regions: the infraorbital fossa, the pterygopalatine fossa and the middle cranial fossa.

The IOF, almost completely closed by the periorbita, transmits the infraorbital nerve and artery, the zygomatic nerve, often an anastomotic vein connecting the inferior ophthalmic vein with the pterygoid plexus (see Chapter 3) and, possibly, some parasympathetic branches to the lacrimal gland coming from the sphenopalatine ganglion (see Chapter 3).

Superolateral Angle

In analogy with the inferolateral angle, also the posterior part of the superolateral angle is occupied by an elongated opening. This is the **superior orbital fissure (SOF)** which represents the largest communication between the orbit and the middle cranial fossa. It is about 22 mm long and its anterior end lies 30–40 mm behind the orbital margin. The fissure, though greatly varying in shape and size among individuals (Fig. 1.13), roughly has the shape of a tennis racket with a larger posterior portion, lying inferomedially, and a superolaterally located thin forward-directed elongated portion (the handle of the racket). The inferior root of the lesser wing of the sphenoid (optic strut) separates the posterior end of the fissure from the optic foramen. The inferior and superior edges of the fissure are bounded by the greater and lesser wings of the sphenoid respectively. Along the inferior margin, at the border between the larger inferomedial and the thinner superolateral portions, the **spina musculi recti lateralis** is often present, a small variably-shaped bony spine (Fig. 1.13) which receives the insertion of the common tendinous ring, the fibrous ring that gives origin to the four recti (see Chapter 4); in particular, a part of the LR takes origin from the spina recti lateralis. The common tendinous ring, also known as annulus of Zinn, partially overlaps with the SOF, crossing its posterior and larger portion twice: the first time ascending vertically from the spina recti lateralis to the superior edge of the fissure, the second time bridging the two edges of the fissure almost horizontally just over the posterior end of the fissure. In this way the annulus of Zinn divides the fissure into intraconal and extraconal spaces: the intraconal space, **oculomotor foramen**, is comprised within the fibrous ring and is crossed by the nasociliary and the abducens nerves, the superior and inferior divisions of the oculomotor nerve, the sympathetic and long roots of the ciliary ganglion, and sometimes the deep recurrent ophthalmic artery (see Chapter 3); the extraconal spaces are just under and above the common tendinous ring (Fig. 1.14). The space under the fibrous ring is very small and occasionally traversed by the inferior ophthalmic vein. The following elements can be found in the space over the annulus of Zinn: the superior ophthalmic vein leaving the orbit, the trochlear, frontal and lacrimal nerves entering it, and frequently two arterial anastomoses crossing it: the meningoophthalmic artery and the anastomosis between the recurrent meningeal branch of the lacrimal artery and the sphenoidal branch of the middle meningeal artery (see Chapter 3). In addition, in about 10% of orbits the superficial recurrent ophthalmic artery (marginal tentorial artery) leaves the orbit through the SOF. In less than 1% of cases (0.74%) a bony bridge is present at the inferomedial extremity of the SOF. This bridge forms a large foramen, referred to as **Warwick's foramen**, which connects the orbital cavity with the middle cranial fossa (Fig. 1.15).

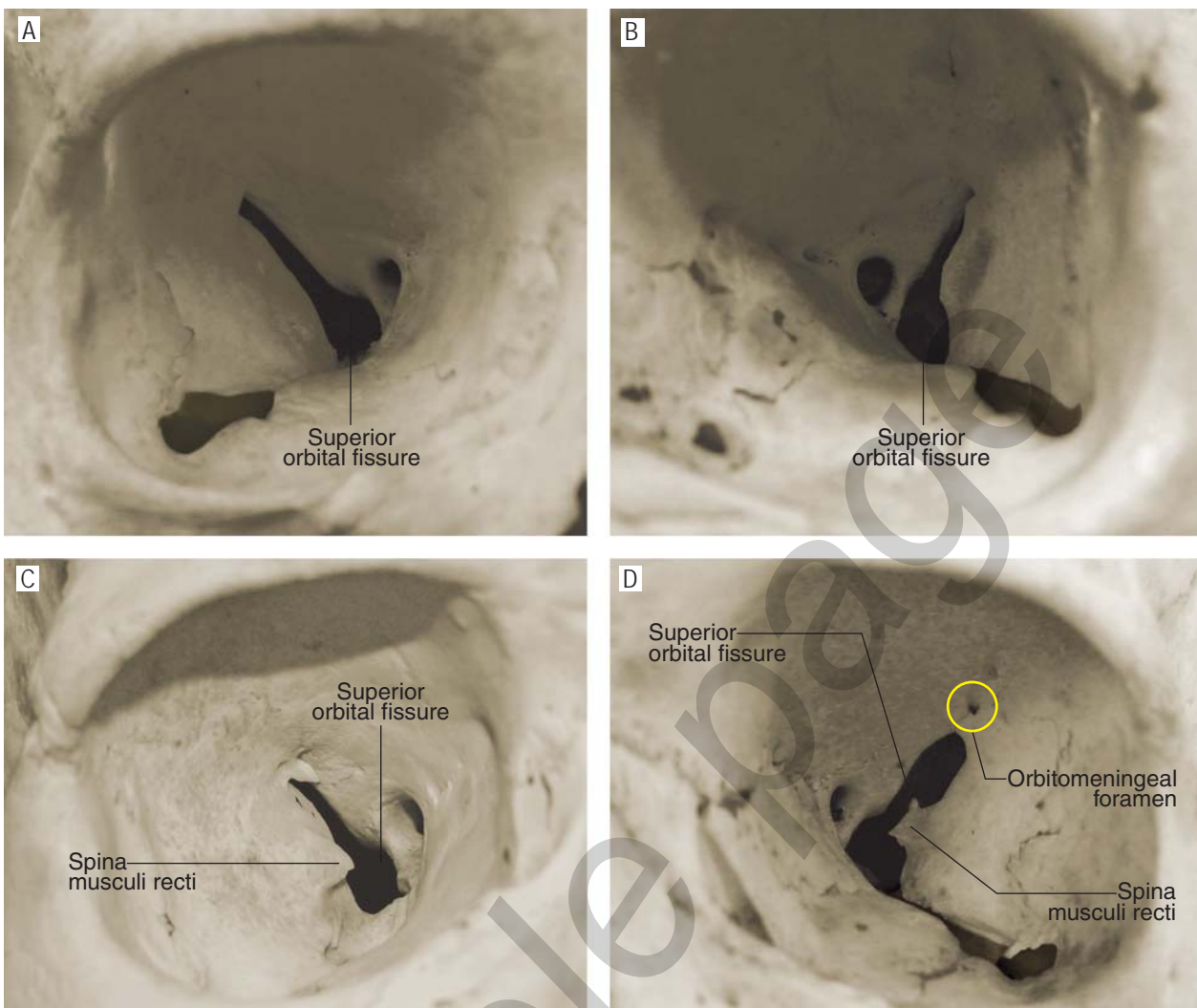


Fig. 1.13 Size and shape variations of the superior orbital fissure and spina musculi recti lateralis. Anterior views of the right (A, C) and left orbits (B, D).

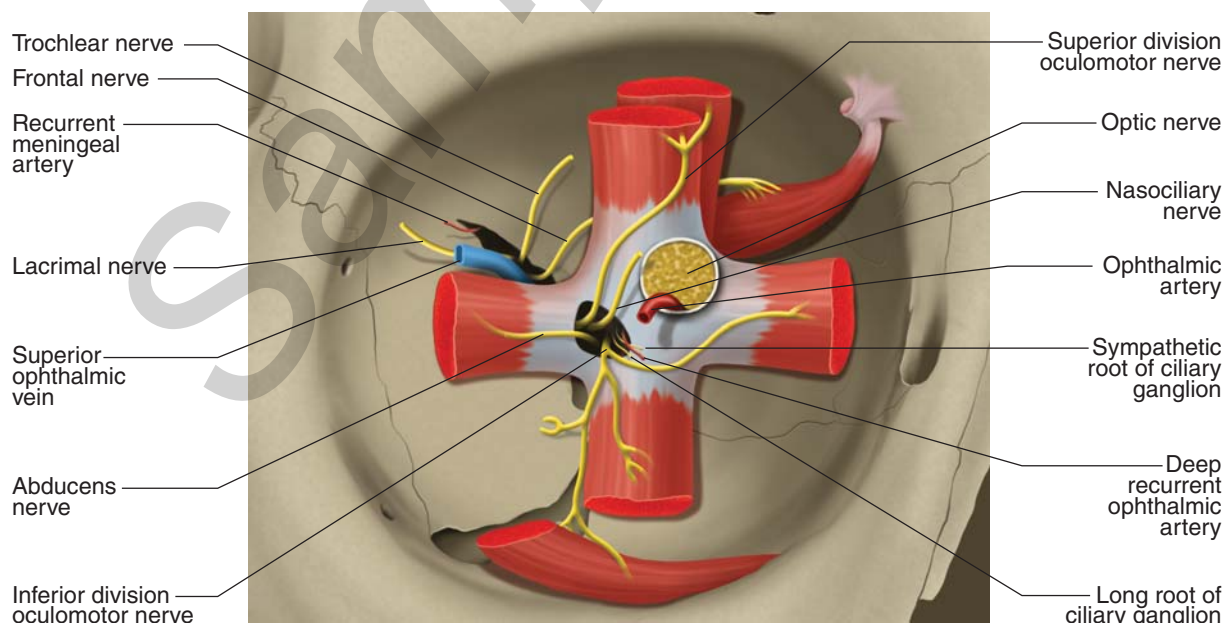


Fig. 1.14 Common tendinous ring and superior orbital fissure. Vessels and nerves passing through the superior orbital fissure.

CHAPTER 2

Eyelids, Conjunctiva, Lacrimal Glands and Ducts

Eugenio Bertelli, Claudio Nicoletti

List of Abbreviations

CALT	Conjunctiva-Associated Lymphoid Tissue	LPL	Lateral Palpebral Ligament
CK	Cytokeratin	M cells	Membranous Epithelial Cells
EALT	Eye-Associated Lymphoid Tissue	MALT	Mucosa-Associated Lymphoid Tissue
EGF	Epidermal Growth Factor	MPL	Medial Palpebral Ligament
LA	Levator Aponeurosis	MRD	Mean Reflex Distance
LDALT	Lacrimal Drainage-Associated Lymphoid Tissue	OrOc	Orbicularis Oculi
LP	Levator Palpebrae Superioris	OS	Orbital Septum
		SPM	Superior Palpebral Muscle
		VIP	Vasoactive Intestinal Peptide

The Eyelids

General Morphology

The eyelids are two mobile fibromuscular folds covered externally by skin and internally by the conjunctiva. Placed in front of the anterior opening of the orbit, they appear convex due to the underlying eyeball bulging forward.

The superior eyelid merges upward with the eyebrow at the **superior orbitopalpebral sulcus**. The inferior eyelid is continuous downward with the skin of the zygomatic region; the shallow **inferior orbitopalpebral sulcus** separates the inferior eyelid from the lid-cheek segment of the midcheek region. It begins close to the medial canthus and runs laterally curving upward to fade in proximity of the lateral canthus (Fig. 2.1). Further downward two additional folds, the shallow **nasojugal** and **palpebromalar folds**, can be seen extending into the midcheek region and marking the inferior border of the lid-cheek. The former begins close to the medial canthus and runs laterally and downward to end below the inferior margin of the orbital opening, the latter courses downwards and medially from below the lateral canthus toward the inferior part of the nasojugal fold (Fig. 2.2).

With their opposed free edges (i.e. lid margins), the superior and inferior eyelids outline the **palpebral fissure**, a 10-12 mm high and 28-30 mm long opening whose ends are known as **medial** and **lateral canthi** (or **angles**) (Fig. 2.1). Through the palpebral fissure, depending on the degree of opening, variable portions of cornea and sclera can be seen. On average the upper lid margin is a couple of millimeters lower in adults than in children where it lies just at the level of the upper limbus; its peak is just medial to a vertical line passing through the center of the pupil. The lower lid margin is tangential to the inferior limbus and its lowest point lies laterally to the vertical line passing through the pupil. The interpalpebral distance is on average 10-12 mm wide. This value can be divided into the mean reflex distance (MRD)

CHAPTER 3

Orbital Vessels and Nerves

Eugenio Bertelli

List of Abbreviations

CRA	Central Retinal Artery	MMA	Middle Meningeal Artery
E-W	Edinger-Westphal	OA	Ophthalmic Artery
E-Wcp	E-W nucleus with centrally projecting cells	ON	Optic Nerve
E-Wpg	E-W nucleus with preganglionic cells	PCA	Posterior Ciliary Artery
IOV	Inferior Ophthalmic Vein	SOV	Superior Ophthalmic Vein
LA	Lacrimal Artery		

Arteries

The arterial blood supply of the orbit derives mainly from the **ophthalmic artery** (OA) (Fig. 3.1). In addition, the orbit receives minor contributions from the **infraorbital artery**, **middle meningeal artery** (MMA) and **anterior deep temporal artery**, branches of the internal maxillary artery, and from the **angular artery**, terminal branch of the facial artery.

Ophthalmic Artery

The OA is the first important branch of the internal carotid artery. It has an average diameter ranging from 1.5 to 1.9 mm. The OA takes origin from the internal carotid artery in about 96%-98% of cases. The site of origin usually coincides with the emergence of the internal carotid artery from the cavernous sinus. In 4% to 8% of cases, however, it arises earlier when the carotid artery is still in the cavernous sinus. In exceptional cases, the OA stems from a higher position, namely from the supraclinoid portion of the internal carotid artery. In a very limited number of individuals (1% to 3% of cases) the OA arises from the MMA, whereas in 2% to 4% of cases its origin is double; in this instance, the thinner OA usually comes from the internal carotid artery whereas the larger one stems from the MMA (Fig. 3.2). Hence, in 3.4% to 6.6% of individuals (depending on the statistical surveys) the territory supplied by the OA falls entirely, or in large part, into the area of distribution of the external carotid artery. A double OA can also be the result of two arteries arising from the internal carotid artery, one from the intracavernous portion and the other from the supraclinoid area. In extremely rare cases, the OA has been reported as stemming from the middle cerebral artery, the anterior cerebral artery, the posterior communicating artery or even the basilar artery.

For descriptive purposes, the course of the OA is divided into intracranial, intracanalicular and intraorbital parts. In its short intracranial course (about 4 mm), the OA runs in the subdural space, between the internal carotid artery, located inferiorly, and the lateral half of the optic nerve (ON) that runs superiorly. At its entrance into

CHAPTER 4

Extraocular Muscles and Intraorbital Connective Tissue

Eugenio Bertelli

List of Abbreviations

IO	Inferior Oblique muscle	MR	Medial Rectus muscle
IR	Inferior Rectus muscle	SIF	Singly Innervated Fiber
LA	Levator Aponeurosis	SO	Superior Oblique muscle
LP	Levator Palpebrae superioris muscle	SPM	Superior Palpebral Muscle
LR	Lateral Rectus muscle	SR	Superior Rectus muscle
MIF	Multiply Innervated Fiber		

Extraocular Muscles

General Features

The orbit contains **six** striated extraocular muscles that serve to ocular movements. Based on their general arrangement, they are divided into **four** recti muscles and **two** oblique muscles. Recti muscles are called **Medial Rectus** (MR), **Lateral Rectus** (LR), **Superior Rectus** (SR), and **Inferior Rectus** (IR). Oblique muscles are called **Inferior Oblique** (IO) and **Superior Oblique** (SO). In addition, the **Levator Palpebrae superioris** (LP), though not involved in ocular movements, is usually described among extraocular muscles due to its intraorbital location, common embryologic development and innervation (Fig. 4.1). Ocular movements take place around the centre of rotation, which is very close to the geometric centre of the eye. They can be described as movements of rotation on the three fundamental axes. A rotation on the vertical axis is called **abduction**, if the direction of the eye is turned toward the temporal side, or **adduction**, if the direction of the eye is turned toward the nasal side. A rotation on the transverse axis is called **depression** (or **infraduction**), if the centre of the cornea moves downward, or **elevation** (or **supraduction**) if it turns upward. A rotation on the sagittal axis is called **intorsion** (or medial rotation) if the twelve o'clock of the cornea moves nasally or **extorsion** (or lateral rotation) if the twelve o'clock of the cornea moves temporally (Fig. 4.2). Even though the eyes rotate frequently on non-fundamental axes, each movement can be easily described as a combination of elementary rotations.

Based on its orientation, the contraction of each muscle induces a main movement around a fundamental axis, which is called **primary action**. The rotations on the remaining axes are called **secondary** and **tertiary actions** (Table 4.1). The primary action (main movement) of the IR, for instance, is to depress the eye; this action being more effective when the eye is abducted. When the eye looks ahead, the IR also acts inducing adduction (secondary action) and extorsion (tertiary action). Both secondary and tertiary actions become more pronounced as the eye becomes

CHAPTER 5

General Features of the Eyeball

Eugenio Bertelli

General Features

The eyeball can be compared with an almost spherical shell housing a nucleus of transparent substances (Fig. 5.1). The shell, in turn, is formed by three concentric membranes, or **tunicae (coats)**, that are structurally and functionally different. The outer membrane is the **fibrous coat** (see Chapter 6), consisting of a larger and opaque posterior portion, the **sclera**, and a transparent less extensive anterior portion, the **cornea**.

The **uvea** (see Chapter 7) is the intermediate membrane and it is a vascular layer. Its posterior 2/3 are in contact with the sclera and are known as the **choroid**. Forward, though still in contact with the sclera, the uvea has a different and more complex structure, due to the presence of the **ciliary muscle**. Along with the inner membrane, this part of the uvea is called the **ciliary body**. The **iris** is the anterior-

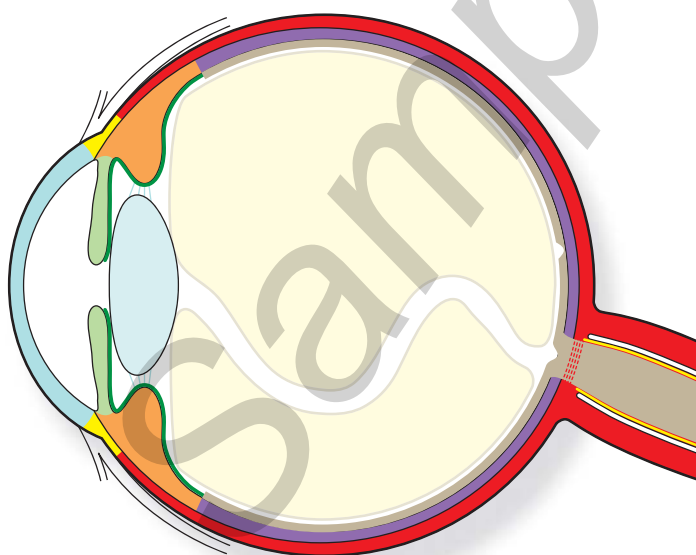


Fig. 5.1 Schematic arrangement of the eye. The eye is formed by a shell of three concentric coats: the outer coat is the fibrous coat and is formed by the sclera (red ♦) and the cornea (light blue ♦). The transition area between sclera and cornea is the limbus (yellow ♦). The second tunica of the eye is the uvea and consists of three segments: choroid (purple ♦), ciliary body (orange ♦), and iris (light green ♦). The innermost coat is the retina which is made of a light sensitive part (brown ♦) and a blind part (dark green ♦) which provides an inner covering to the ciliary body and to the iris. The eye shell contains the lens (light sky blue ♦), just behind the iris, the humor aqueous (white), in front of the iris and around the lens and the vitreous (beige ♦), behind the lens.

CHAPTER 6

Fibrous Tunica: Cornea, Sclera and Corneoscleral Limbus

Eugenio Bertelli, Claudio Traversi, Cosimo Mazzotta, Giulia Borsari

List of Abbreviations

CGRP	Calcitonine Gene-Related Peptide	SP	Substance P
CK	Cytokeratin	TEM	Transmission Electron Microscopy
FGF	Fibroblast Growth Factor	TGF β	Transforming Growth Factor B
JT	Juxtaganicular Tissue	TM	Trabecular Meshwork
NPY	Neuroactive Peptide Y	VAChT	Vesicular Acetylcholine Transporter
PDGF	Platelet Derived Growth Factor	VIP	Vasoactive Intestinal Peptide
SC	Schlemm's Canal		

The fibrous tunica (fibrous coat) is the outer layer of the eyeball. Its consistency gives a minor contribution to the stiffness of the eye which is mainly due to the positive inner pressure. The **cornea**, the anterior sixth of the fibrous coat, is transparent. The posterior 5/6, the **sclera**, are opaque and white. The 1.5-2 mm wide transition zone between the cornea and the sclera is referred to as the **corneoscleral limbus** (Fig. 6.1). On the inner side, the corneoscleral limbus houses a series of structures that are involved in the reabsorption of the aqueous humor from the anterior chamber.

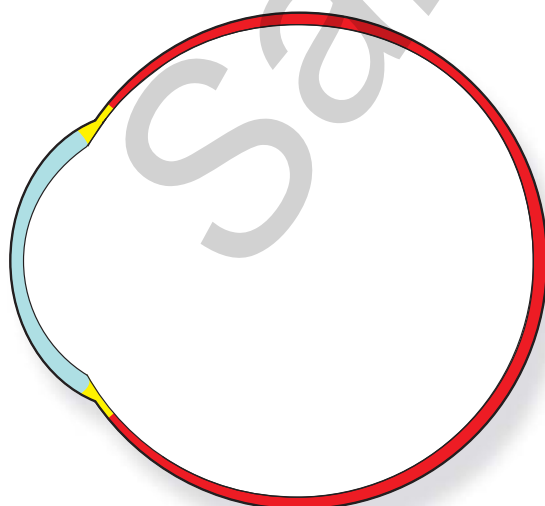


Fig. 6.1 The outer tunica of the eye is the fibrous coat. The posterior part is the sclera (red ♦) whereas its anterior part is the cornea (light blue ◆). The transition between sclera and cornea is the corneoscleral limbus (yellow ♦).

CHAPTER 7

Vascular Tunica: Choroid, Ciliary Body and Iris

Eugenio Bertelli, Paolo Toti

List of Abbreviations

CC	Choriocapillaris	OS	Ora Serrata
CGRP	Calcitonin Gene-Related Peptide	PDGF	Platelet Derived Growth Factor
CK	Cytokeratin	SMC	Smooth Muscle Cell
CNPE	Ciliary Nonpigmented Epithelium	SP	Substance P
CPE	Ciliary Pigmented Epithelium	TEM	Transmission Electron Microscopy
JT	Juxtaganicular Tissue	TGF β	Transforming Growth Factor β
nNOS	Neuronal Nitric Oxide Synthase	TM	Trabecular Meshwork
NO	Nitric Oxide	VAcH T	Vesicular Acetylcholine Transporter
NPY	Neuroactive Peptide Y	VIP	Vasoactive Intestinal Peptide
NVSMC	Non-Vascular Smooth Muscle Cell		

General Features

The vascular tunica of the eyeball, the **uvea**, is interposed between the nervous and the fibrous coats. The latter, on the other hand, is strictly apposed to the uvea only with its scleral segment. The name uvea derives from the grape-like look that the tunica acquires when isolated from the sclera.

The uvea consists of three portions, each in continuity with the other, with different structure and function. From behind forward the uvea comprises the **choroid**, the **ciliary body** and the **iris** (Fig. 7.1).

Choroid

The choroid represents the posterior 2/3 of the vascular coat (Fig. 7.1) and, extending forward from the optic nerve to the ora serrata (OS), it shares the same limits of the light-sensitive part of the retina (see Chapter 8). It is mainly formed by vessels that guarantee the metabolic exchange between blood and the outer layers of the retina. In human beings, 90% of oxygen required by the retina comes from the choroid circulation and 90% of all the oxygen delivered to the retina is used by photoreceptors. To accomplish such demanding task despite the presence of barriers like Bruch's membrane (see p. 162-163) and the retinal pigmented epithelium, a steep gradient of oxygen tension between the choroid and the retina has to be kept constant. This is achieved by a very high level of blood flow, possibly the highest in the body per unit of tissue weight. It has been estimated that such flow, close to 1200 ml/min/100g, is about 10 folds higher than in the brain. Thanks to this substantial blood flow, oxygen tension in the choroid is maintained high with the arterial/venous difference of only 3% versus 38% for the retinal circulation. The latter one

CHAPTER

8

Retina

Eugenio Bertelli, Ivanela Kondova, Jan A.M. Langermans

List of Abbreviations

BB	S-Cone Bipolar = Blue Bipolar	M-Cone	Medium wavelength Cone
DB	Diffuse Bipolar	Me-Cone	Melanopsin Cone
FMB	Flat Midget Bipolar	MG	Midget Ganglion
GABA	Gamma-Aminobutyric Acid	PG	Parasol Ganglion
GB	Giant Bipolar	PKC	Protein Kinase C
GP	Glycogen Phosphorylase	RB	Rod Bipolar
IMB	Invaginating Midget Bipolar	RHAMM	Receptor for Hyaluronan Mediate Motility
ipG	Intrinsically photosensitive Ganglion	S	Stratum/Strata
IRBP	Interphotoreceptor Retinoid-Binding Protein	SBG	Small Bistratified Ganglion
L-Cone	Long wavelength Cone	S-Cone	Short wavelength Cone
LGN	Lateral Geniculate Nucleus	SMG	Smooth Monostratified Ganglion

General Features

The retina develops from the primitive optic cup (see Chapter 14). Due to the same embryologic origin, the epithelial lining of the ciliary body and the iris epithelium should also be considered part of the retina. Indeed, in many textbooks a division is frequently proposed between the light-sensitive and the blind parts of the retina, the latter being that portion of the retina anterior to the ora serrata and corresponding to the ciliary and iris epithelia. Nowadays, it is customary to consider the retina only the portion extending behind the ora serrata (Fig. 8.1). It should be noted, however, that such approach is not justified, either from an embryologic or anatomic viewpoint, since the continuity between these two portions is maintained even when their development is complete. On the other hand, as the retina, in a clinical context, is usually identified exclusively with its light-sensitive portion, from now on this chapter will conform with this view, the blind portion of the retina having been already dealt with in the paragraphs dedicated to the iris and the ciliary body (see Chapter 7).

The retina is a delicate and thin layer of nervous tissue. The retina anterior border, beyond which it continues with the ciliary epithelium, is marked by the ora serrata, whereas its posterior limit corresponds to the edge of the optic disc, though its nerve fiber layer (see p. 241-242) extends into the optic disc where it forms the optic nerve. The retina is made up by two concentrically arranged main layers: the pigmented epithelium, externally placed and developed from the primitive optic cup outer layer, and the sensory layer, characterized by a highly complex nervous structure and derived from the optic cup inner layer.

thinness, it does not allow an efficient electrotonic conduction either. Thus, H1 cell telodendron results electrically isolated from the dendritic arborization. The two parts of the cell, therefore, possibly act as independent units that receive and integrate autonomously inputs coming from cones and rods. H1 cells are more numerous in the fovea, where their density is about 25,000 cells/mm²; while such density drastically decreases towards the periphery, where it is 1000 cells/mm². Even their morphology changes according to eccentricity. In peripheral retina, H1 cells have long and scarcely ramified dendrites; overall the dendritic tree measures 160 µm in diameter and makes contact with about 50 pedicles. In contrast, in the fovea H1 cell dendrites are shorter and highly branched, covering an area that measures 16 µm in diameter and contacting only 6-7 pedicles (Fig. 8.27). In the fovea the receptive field of H1 cells coincides with the size of the dendritic tree, whereas in the periphery it is considerable larger (309 µm at 11 mm of eccentricity). This difference could be due to a different degree of electric coupling among adjacent cells; in other words H1 cells of the peripheral retina could be more extensively joined through gap junctions.

In contrast to the axon-bearing H1 cells, H2 cells have smaller nuclei and are axonless. They have a local broad dendritic arborization and one or two axon-like longer dendrites (100-300 µm in length) lacking terminal ramifications. H2 cell dendrites receive inputs from all cones but they converge mainly on S-cone pedicles (Fig. 8.27).

On the whole, therefore, dendrites of horizontal cells, either H1 or H2, are postsynaptic to cone pedicles, whereas the axons of H1 cells are postsynaptic exclusively to rod spherules. Studies carried out on monkey retinas show that each pedicle is in contact with 3-5 H1 and 3-5 H2 horizontal cells. As we have already mentioned (see p. 209) horizontal cells are provided with AMPA ionotropic (coupled to ion channels) glutamate receptors. The pattern of glutamate receptors is slightly different according to the horizontal cell type: both H1 and H2 cells are provided with AMPA GluR2-4 receptors on the dendrites, taking part to the tetrads and on the desmosome-like junctions. In addition, however, H1 cells also have KA GluR6/7 receptors on desmosome-like junctions. In absence of luminous stimulation, glutamate binding to receptors keeps cationic channels open and maintains horizontal cells in a state of partial depolarization. By decreasing glutamate release, luminous stimulation on photoreceptors induces horizontal cell hyperpolarization. This response is achieved on H1 cells by stimulations with green or red light, whereas H2 cells show the same response with luminous stimulations with green, red or blue light. Hence, no selectivity has been found for L- or M-cone inputs in H1 cells and even less selectivity has been found for H2 cells, as they hyperpolarize in the same way by stimulating all types of cones.

Horizontal cells have not a center-surround receptive field organization (the response has always the same sign, whichever area of the receptive field is stimulated); in addition, even though H1 and H2 cells show different connectivity with cones (H2 cells preferentially contact S-cones, H1 cells tend to skip S-cones), their response to luminous stimulation is not color opponent.

Horizontal cells are thought to produce and release GABA. The nearest cognate receptors are located on cone pedicles and on bipolar cell dendrites. So far, it is not clear how horizontal cells achieve GABA secretion as well as the exact influence that, at this level, GABA exerts on the transmission of visual information. Nevertheless, even though the precise synaptic mechanisms are not known, the prevalent opinion is that, on the whole, horizontal cells function is to shape the antagonistic periphery of cones and bipolar cell receptive fields. As RB cells (see p. 217) do not possess a center-surround receptive field structure, the role played by H1 horizontal cells in the tetrads of the spherules is possibly different.

Bipolar Cells

Retinal bipolar cells form a heterogeneous population of about 35,000,000 glutamatergic neurons. They are 2nd order sensory conducting neurons that transmit visual information from photoreceptors to ganglion and amacrine cells. The cell body

of bipolar cells is as large as 9 μm in the fovea and 5 μm in more peripheral areas. Bipolar cell nuclei account for 40% of the nuclei in the inner nuclear layer. Two cytoplasmic processes extend from the cell body of bipolar cells in opposite directions (Fig. 8.28): one dendrite, distributing to the outer plexiform layer, and one axon that enters the inner plexiform layer. From an ultrastructural viewpoint all bipolar cells show the same general features consisting of a rounded or oval-shaped nucleus with one or two nucleoli, a well-developed Golgi complex located near the origin of the primary dendrite, a prominent rough endoplasmic reticulum, mitochondria and free ribosomes. Dendrites have a section diameter as large as 0.1-0.2 μm at the fovea and they contain microtubules, numerous slender mitochondria and a few vesicles. The axon, provided with microtubules, vesicles and very rare mitochondria, is surrounded by Müller cells cytoplasmic processes up to the inner plexiform layer where it forms its telodendron. The telodendron ends into synaptic terminals containing large mitochondria and synaptic vesicles mainly gathered around synaptic ribbons. Synaptic ribbons in bipolar cells are smaller, usually lacking the arciform density,

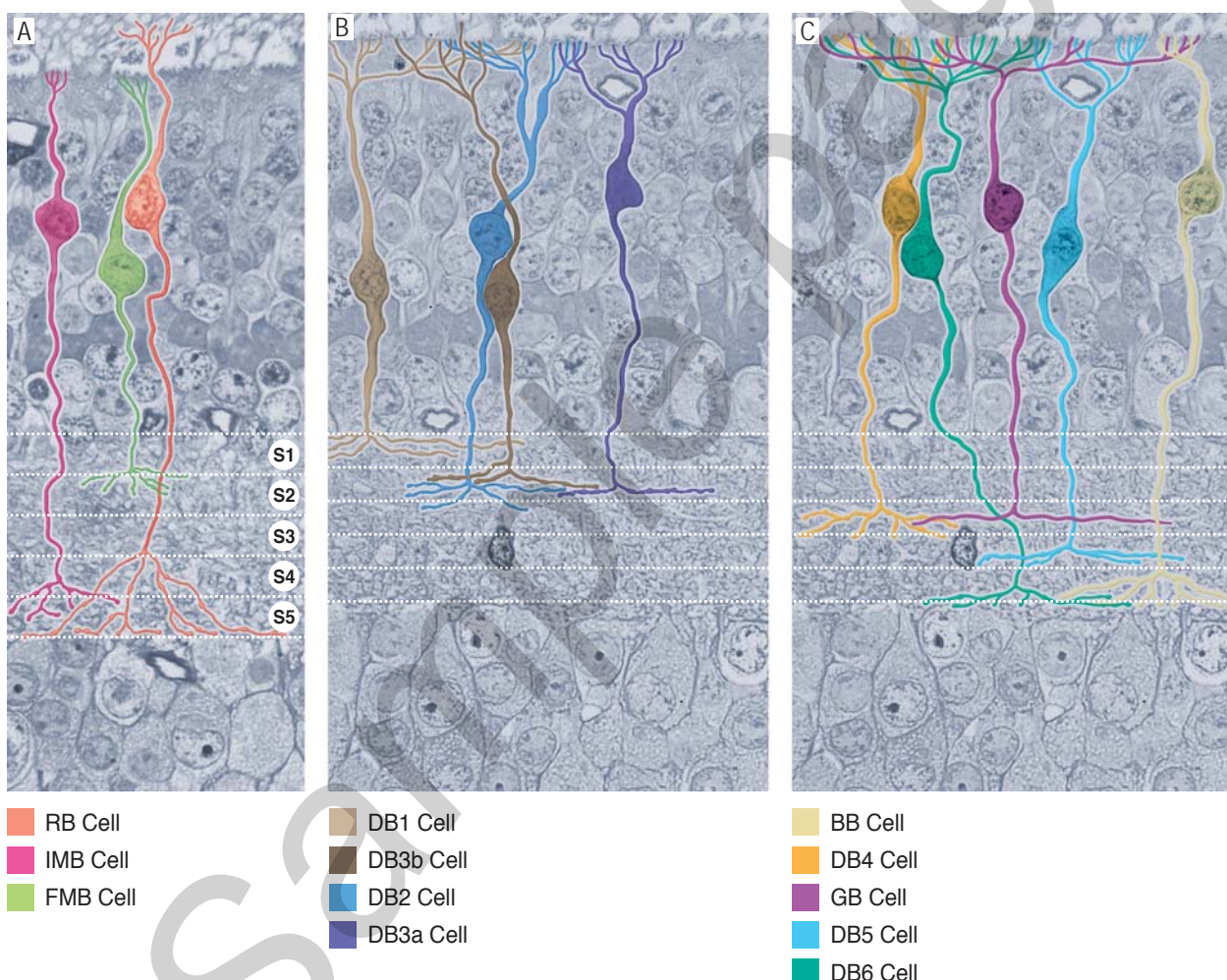


Fig. 8.27 Retina. Morphology and level of axon terminal ramifications of the different types of bipolar cells. A) Rod bipolar (RB) cells (orange) collect inputs from rod spherules and ramify in S5; invaginating midget bipolar (IMB) cells (lilac) gather inputs from single pedicles and ramify their axons in S4-S5; flat midget bipolar (FMB) cells (light green) collect inputs from single pedicles and their axons end in S1-S2. B) OFF-center diffuse bipolar (DBa) cells. DB1 cells (light brown) receive inputs from all pedicles within their dendritic tree. They end distributing their axon terminals in S1; DB2 cells (blue) collect inputs from all pedicles within their dendritic tree. Their axon terminals are located in S1-S2; DB3a cells (dark blue) gather visual information mainly from M- and L-cones. Their axons distribute within a narrow stripe of S2; DB3b cells (dark brown) collects inputs from cone pedicles and also from a few spherules. Their axonal distribution overlaps that of DB3a cells. C) ON-center diffuse bipolar (DBb) cells, giant bipolar cells (GB) and S-cone bipolar cells (BB). DB4 cells have a dendritic tree which collects inputs mainly from M- and L-cones. Their axon terminals distribute within S3 (orange); DB5 cells (light blue) collect inputs exclusively from M- and L-cones. Their axon radiates within a narrow stripe of S4; DB6 cells (turquoise) have a broad dendritic tree which gathers inputs from all types of cones. Their axon distributes to S5; GB cells (purple) have a large and sparse dendritic tree which collects inputs only from half pedicles. Their axon ends within S3; BB cells (beige) collects inputs from 2-3 S-cones. Their axon arborizes in S5.

and more numerous (30 to 50) than in photoreceptor cells. It is usually assumed that bipolar cells signal through graded depolarization. It has been recently shown, however, that a few types of bipolar cells can generate action potentials.

Taking into account connections and branching patterns of dendrites and axons, 12 types of different bipolar cells have been described so far (Fig. 8.28). The first major feature that is used to classify bipolar cells refers to the kind of photoreceptors to which they are postsynaptic. Based on this criterion, **rod bipolar cells** are distinguished from **cone bipolar cells**. Whereas the former type of bipolar cells makes up a homogeneous population, the latter type is further classified in at least three major subpopulations (Fig. 8.28): i) **midget bipolar cells**, which may be split into either **ON-center** or **OFF-center** subtypes; ii) **diffuse bipolar cells**, divided into three **ON-center** and four **OFF-center** subtypes; iii) **S-cone bipolar cells**. In addition, **giant bipolar cells** have been recently described, but data on this variety are still poor and we will deal with it only briefly.

Rod Bipolar Cells

Rod bipolar cells (RB) are about 20% of all bipolar cells. RB cells are not present in the fovea and they appear only at 1 mm of eccentricity from the foveal center. On average, RB cell body is 10 μm large and it is located in the outer half of the inner nuclear layer, sometimes among the perikarya of horizontal cells on the border of the outer plexiform layer. The cell body gives origin to a robust dendrite that enters the outer plexiform layer ramifying repeatedly and eventually dividing into a series of pointed terminal branchlets, whose number varies as a function of retinal eccentricity. In the area centralis, the dendritic field of RB cells covers a circular surface that measures about 20 μm in diameter, whereas in the peripheral retina this diameter doubles. Each terminal branchlet occupies the central position of a tetrad housed in the deep invagination of a spherule (see p. 205-206). In this way, it is believed that one RB cell makes contact with 30-35 spherules in the area centralis and with 45-50 in the peripheral retina; there are, however, different estimations and according to some investigators the number of rod spherules contacted by each RB cell could be as high as 80-120. RB cell dendrites are provided with APB-sensitive mGluR6 metabotropic glutamate receptors. When engaged by the ligand, these receptors activate a second messenger that closes cationic channels. Without luminous stimulation, when glutamate release from rods saturates the receptors, cationic channels are closed and RB cells are in a hyperpolarized state. The decrease in glutamate release evoked by a luminous stimulation desaturates the receptors. Consequently, cationic channels open allowing an influx of positive ions that depolarizes RB cells. From a functional viewpoint, therefore, synapses between spherules and RB cells are sign-inverting synapses; in addition, all RB cells are ON bipolar cells as they depolarize to increments of light.

The axon of RB cells dives into the *sublamina b* of the inner plexiform layer (see p. 232-235) without giving off collaterals. Once reached S5, the deepest stratum of the inner plexiform layer (see p. 228), it gives origin to numerous telodendria that resolve into few large terminals housing synaptic ribbons and glutamate-containing synaptic vesicles (Fig. 8.28). The postsynaptic elements of RB cell ribbon synapses are almost always two dendrites of amacrine cells, one belonging to an AII cell and one to an A17 cell (see p. 223-225). It has been estimated that only in 0.3% of cases one or both postsynaptic elements derive from ganglion cells. Regardless of the identity of their constitutive elements, the postsynaptic complexes formed by two dendritic processes are known as **diads**. Rarely, it is possible to observe a single postsynaptic element (**monad**) that invariably belongs to an amacrine cell. RB cell axonal terminals also act as postsynaptic elements of conventional synapses with amacrine cells. The synaptic output/input ratio in RB cell axons is 0.5. RB cells express some proteins, like **protein kinase C (PKC) α** , **calcium-binding protein-5, Islet-1** transcription factor, and **protein G $_{\alpha\alpha}$** , that have been proposed as molecular markers. Unfortunately, these proteins are not exclusive of RB cells and they are even expressed in one type of diffuse bipolar cells.

RB cell receptive field seems to be an exception among bipolar cells. Whereas

CHAPTER 9

Aqueous Humor, Lens Ciliary Zonule, Vitreous

Eugenio Bertelli

List of Abbreviations

MAGP	Microfibril Associated Glycoprotein
------	-------------------------------------

The dioptric media of the eye include the **tear film**, the **cornea**, the **aqueous humor**, the **lens** and the **vitreous**. The tear film and the cornea have been previously dealt with in Chapters 2 and 6 respectively. This chapter is dedicated to the following items: aqueous humor, lens and vitreous. The ciliary zonule is described together with the lens.

Aqueous Humor

The aqueous humor is a perfectly transparent fluid that occupies the two chambers of the eye. It has a specific weight very close to water (1.006) and it is slightly acidic ($\text{pH} = 7.21$) compared to blood pH. Its refraction index is 1.333. The aqueous humor is produced by the ciliary processes in the posterior chamber (see Chapter 7), with a circadian rhythm (2.61 $\mu\text{l}/\text{min}$ by day, 1.08 $\mu\text{l}/\text{min}$ by night). It is reabsorbed, mainly through the drainage angle, from the anterior chamber and, in a minor proportion, through the uveoscleral pathway (see Chapter 6). The aqueous humor is an electrolytic solution containing several organic molecules, such as growth factors, cytokines and many other proteins. These substances meet the metabolic needs of the avascular tissues present in the anterior segment of the eye and they may even play a role in the regulation of intraocular pressure (about 20-25 mm/Hg).

Some ions in the aqueous humor have concentrations similar to those encountered in plasma (Na^+ , K^+ , Mg^{++}), whereas the concentration of other ions is quite different; Cl^- , for instance, is more concentrated in the aqueous humor (131 $\mu\text{mol}/\text{ml}$) than in plasma (107 $\mu\text{mol}/\text{ml}$), whereas HCO_3^- ion concentration is higher in plasma than in the aqueous humor (26 $\mu\text{mol}/\text{ml}$ vs. 22 $\mu\text{mol}/\text{ml}$). Other significant differences concern lactic acid concentration, which, in the aqueous humor, is more than double (4.5 $\mu\text{mol}/\text{ml}$) compared to plasma (1.9 $\mu\text{mol}/\text{ml}$), and ascorbic acid concentration, which is 25 folds higher (1.06 $\mu\text{mol}/\text{ml}$) than in plasma (0.04 $\mu\text{mol}/\text{ml}$). In contrast, glucose concentration is higher in plasma (5.9 $\mu\text{mol}/\text{ml}$) than in the aqueous humor (2.8 $\mu\text{mol}/\text{ml}$) and only traces of free amino acids are present

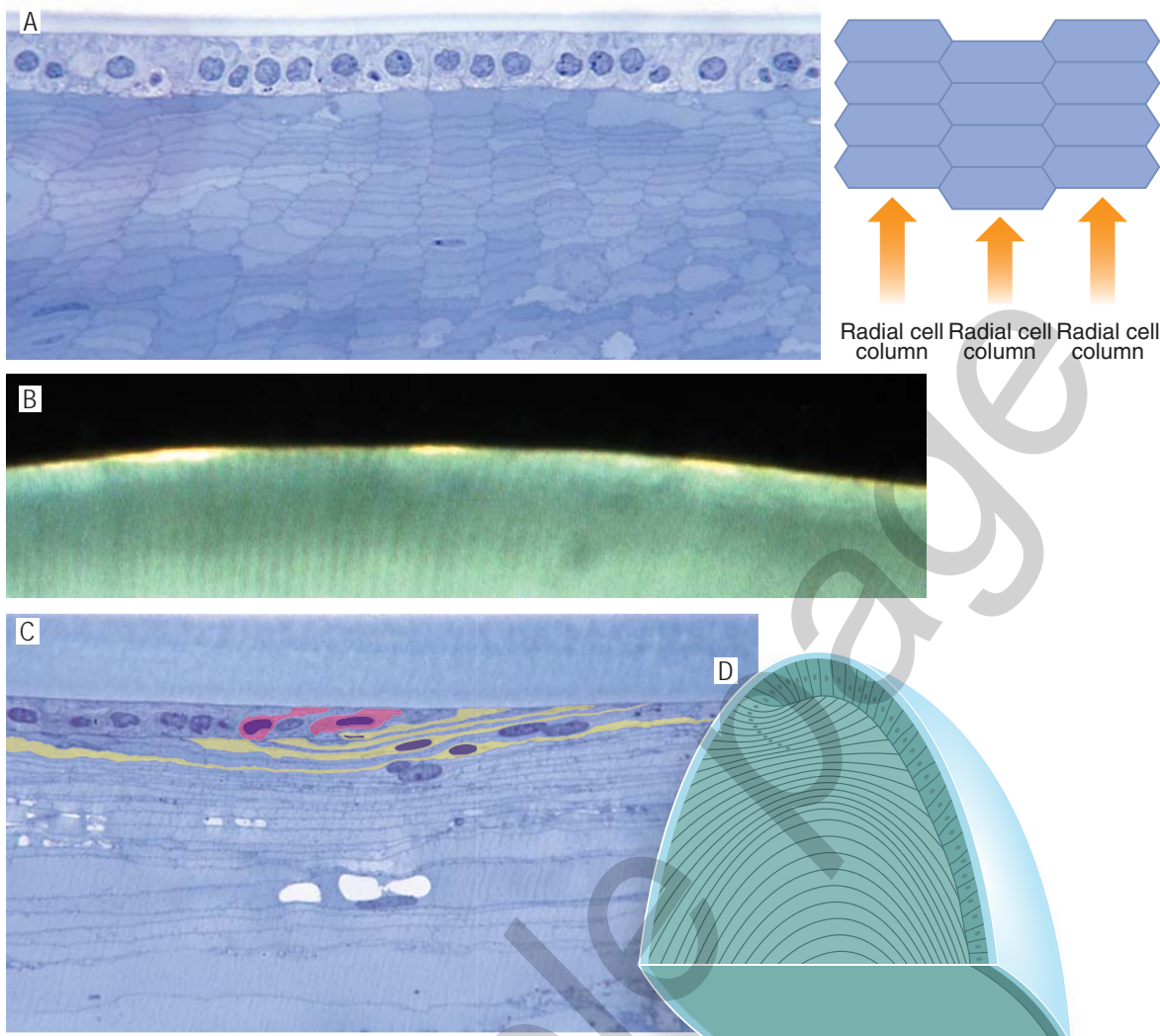


Fig. 9.7 Lens fibers. A) Histologic feature of lens fibers and their general arrangement. Frontal section of the lens. Lens fibers show a hexagonal profile and are piled one over the other forming radial cell columns. B) Incident light on the surface of the lens shows the most superficial fibers of the meridionally oriented radial cell columns. *Macaca Mulatta*. C) Elongating fibers in the transition zone. Meridional section of the lens. Cells of the anterior epithelium, on the left of the figure, moving posteriorly (towards the right of the figure) progressively get taller and taller and incline the major axis so that they appear as lying down beneath the anterior epithelium. Some cells have been highlighted to better appreciate their progressive growth. *Macaca Mulatta*. D) Schematic drawing of the lens anterior epithelium and fibers sectioned along a meridional plane. The arrangement of the elongating fibers nuclei draws a sort of arch, the nuclear bow.

whereas the youngest fibers form arches with a slight outward concavity, those a little older are almost straight and those further older make arches with the concavity directed towards the lens axis. Such concavity results the more pronounced the longer and older the fibers are (Fig. 9.7).

So far we have described what happens to cells belonging to a single meridional row of the transitional zone. Now, let us see what occurs to the cells that are generated at the same time in all the meridional rows of the transitional zone. These cells lie one beside the other and they will become a single generation of lens fibers to which each radial cell column contributes with a single element. Each generation of elongating fibers form a **growth shell**, a sort of incomplete sheath extending from the anterior to the posterior face of the lens and straddling the equator. Growth shells are not static structures but, with the elongation of their fibers, they gradually expand along the lens faces toward the poles. Their completion is achieved only when they have entirely wrapped the deeper layers. In other words, successive generations of elongating fibers form concentric growth shells that are the more complete the older and the deeper they are (Fig. 9.8).

CHAPTER 10

Intraocular Visual Pathway: Intraretinal Circuitry

Eugenio Bertelli

List of Abbreviations

BB	S-Cone bipolar = Blue Bipolar	M-Cone	Medium wavelength Cone
DB	Diffuse Bipolar	MG	Midget Ganglion
DBa	OFF-Center Diffuse bipolar	PG	Parasol Ganglion
DBb	ON-Center Diffuse bipolar	RB	Rod Bipolar
ipG	Intrinsically photosensitive Ganglion	SBG	Small Bistratified Ganglion
L-Cone	Long wavelength Cone	S-Cone	Short wavelength Cone
LGN	Lateral Geniculate Nucleus		

General Features

The visual pathway consists of a series of specialized nervous formations which gather, transfer and integrate visual information. The visual pathway, therefore, begins with photoreceptor cells and ends in the brain cortex.

This chapter deals with the intraocular part of the visual pathway, which is formed by the intraretinal circuits that preside over the first level of integration of the visual information. In the retina, photoreceptor stimulation is spatially and temporally integrated and the graded variations of membrane potential of photoreceptor cells are coded into trains of action potentials that leave the eyeball via the optic nerve.

The fibers of the optic nerve are, for the most part, axons of retinal ganglion cells. As we have already noted (see Chapter 8), the retina is characterized by several populations of ganglion neurons, each one consisting of cells similar in shape and synaptic connectivity. Each population of ganglion cells is distributed throughout the retina to form a regular mosaic. Every ganglion element represents a single tile of the mosaic. In doing so, the dendritic tree of each population of ganglion cells covers the entire retinal surface. The diverse connections and kinetics of response to the luminous stimulations define each population of ganglion cells as a pathway through which a particular aspect of the visual information leaves the eyeball and is transmitted centrally. Though our understanding is still largely incomplete, it is evident that a number of parallel pathways, likely equal to the number of ganglion cell populations, take origin from the retina and project to extraocular nervous targets. Not all these pathways have been characterized. The three best known are: the **midget ganglion (MG) cell pathway**, also referred to as **parvocellular pathway**, since it projects to the parvocellular layers of the lateral geniculate nucleus (LGN); the **parasol ganglion (PG) cell pathway**, also known as **magnocellular pathway**, since it targets the magnocellular layers of the LGN; the **small bistratified ganglion (SBG) cell pathway**, also referred to as the **koniocellular pathway**, since it ends in the koniocellular layers of the LGN (see Chapter 11). The shaping of these pathways begins already at the level of photoreceptors, rods and cones, which operate differ-

CHAPTER 11

Extraocular Visual Pathway

Eugenio Bertelli, Paolo Toti

List of Abbreviations

CO	Cytochrome Oxydase	Pip	posterior nucleus of the Inferior Pulvinar
hMT+(V5)	Human Middle Temporal area (Visual area 5)	PL	Lateral Pulvinar
hV4	human Visual area 4	PLdm	dorsomedial nucleus of the Lateral Pulvinar
IPS	IntraParietal Sulcus	PLvl	ventrolateral nucleus of the Lateral Pulvinar
LGN	Lateral Geniculate Nucleus	PM	Medial Pulvinar
LO	Lateral Occipital complex	TO	TemporoOccipital area
NOT	Nucleus of the Optic Tract	V1	Primary Visual area (striate cortex, visual area 1)
OC	Optic Chiasma	V2	Visual area 2
ON	Optic Nerve	V2d	dorsal Visual area 2
OT	Optic Tract	V2v	ventral Visual area 2
PA	Anterior Pulvinar	V3	Visual area 3
PHC	Parahippocampal Cortical area	V3A	Visual area 3A
PI	Inferior Pulvinar	V3B	Visual area 3B
Plc	central nucleus of the Inferior Pulvinar	V3d	dorsal Visual area 3
Plcl	central lateral nucleus of the Inferior Pulvinar	V3v	ventral Visual area 3
Plcm	central medial nucleus of the Inferior Pulvinar	V7	Visual area 7
Plm	medial nucleus of the Inferior Pulvinar	VO	Ventral Occipital cortex

Visual information, partially integrated within the eye by intraretinal circuitry (see Chapter 10), leave the eye via the optic nerve. Though building up within the eyeball, the optic nerve is mainly located outside the globe. The two optic nerves represent the first portion of the extraocular visual pathways. The extraocular visual pathway of each side includes the following nervous structures (Fig. 11.1):

- 1) optic nerve (ON)
- 2) optic chiasma (OC)
- 3) optic tract (OT)
- 4) lateral geniculate nucleus (LGN)
- 5) geniculocalcarine tract
- 6) primary visual area (striate cortex, visual area 1) (V1)
- 7) extrastriate visual areas (association visual areas)
- 8) pulvinar

CHAPTER 12

Anatomy of the Oculomotor and Palpebromotor System

Eugenio Bertelli

List of Abbreviations

AOS	Accessory Optic System	NRI	Nucleus Raphe Interpositus
CCN	Central Caudal Nucleus	NRPC	Nucleus Reticularis Pontis Caudalis
CEF	Cingulate Eye Field	NRPO	Nucleus Reticularis Pontis Oralis
CGRP	Calcitonin Gene-Related Peptide:	NRTP	Nucleus Reticularis Tegmenti Pontis
cMRF	Central Mesencephalic Reticular Formation	OKNM	Optokinetic Reflexive Movement
dLVN	Dorsal part of the LVN (Deiter's nucleus)	OPNs	Omnipause Neurons
EBNs	Excitatory Burst Neurons	PEF	Parietal Eye Field
E-W nucleus	Edinger-Westphahl nucleus	PFEF	Prefrontal Eye Field
E-Wpc	E-W nucleus with centrally projecting cells	PMT	Paramedian Tract
E-Wpg	E-W nucleus with preganglionic cells	pMVN	Parvocellular component of the MVN
FEF	Frontal Eye Field	PON	Pretectal Olivary Nucleus
hMT+	Middle Temporal area	PPRF	Paramedian Pontine Reticular Formation
IBNs	Inhibitory Burst Neurons	RIMLF	Rostral Interstitial nucleus of the Medial Longitudinal Fasciculus
III nucleus	Oculomotor nucleus	SC	Superior Colliculus
INC	Interstitial Nucleus of Cajal	SEF	Supplementary Eye Field
IO	Inferior Oblique	SIF	Singly Innervated Fiber
IR	Inferior Rectus	SLBNs	Short-Lead Burst Neurons
IV nucleus	Trochlear nucleus	SNC	Substantia Nigra pars compacta
IVN	Inferior Vestibular Nucleus	SNI	Substantia Nigra pars lateralis
LGN	Lateral Geniculate Nucleus	SNr	Substantia Nigra pars reticulata
LLBNs	Long-Lead Burst Neurons	SOA	Supraoculomotor Area
LP	Levator Palpebrae	SP	Substance P
LR	Lateral Rectus	SPEM	Smooth Pursuit Eye Movement
MIF	Multiply Innervated Fiber	SR	Superior Rectus
mMVN	Magnocellular component of the MVN	SVN	Superior Vestibular Nucleus
MR	Medial Rectus	V1	Primary Visual area
MVN	Medial Vestibular Nucleus	VI nucleus	Abducens nucleus
NDP	Nucleus Dorsalis Paragigantocellularis	VII nucleus	Facial nucleus
NOT	Nucleus of the Optic Tract	vLVN	Ventral part of the Lateral Vestibular Nucleus
NPC	Nucleus of the Posterior Commissure	VOR	Vestibulo-Ocular Reflex
NPH	Nucleus Prepositus Hypoglossi	VORM	Vestibulo-Ocular Reflexive Movement
NRG	Nucleus Reticularis Gigantocellularis		

General Features

Eye movements, promoted by extraocular muscle contraction, are under the direct control of three nuclei of gray matter in the brainstem: the **oculomotor (III) nucleus**, the **trochlear (IV) nucleus** and the **abducens (VI) nucleus** (see Chapter

CHAPTER 13

Topographic Anatomy of the Orbit

Eugenio Bertelli

List of Abbreviations

ON	Optic Nerve
OA	Ophthalmic Artery

General Features

The orbit is the small region of the human body that houses the eyeball. It is also densely populated by muscular, nervous and vascular structures. Indeed, it is the high number of vascular and nervous elements enclosed in such a small space that makes the anatomo-topographic study of the orbit an issue of great interest for surgeons. The anterior border of the orbital region is marked by the **orbital septum**. The structures lying in front of the orbital septum are pertinent to the eyelids (see Chapter 2) and will not be considered in this chapter. The structures located behind the septum, though in some cases extending into the eyelids, belong to the orbital region and will be dealt with in the following paragraphs.

A frontal section passing through the mid-orbit shows two main compartments (Fig. 13.1): one is central, the **intramuscular cone** (see Chapter 4), and is arranged along the longitudinal axis of the orbit. As it is outlined by the four recti this space is also referred to as the **muscular pyramid**. The second compartment, **extraconal space**, surrounds the former one and intervenes between the intramuscular cone and the orbit walls. Both compartments are filled with an adipose atmosphere that forms the adipose body of the orbit.

The intramuscular cone has the shape of a truncated cone with the lesser base corresponding to the annulus of Zinn facing backward and medially. The forward-directed greater base is concave as it embraces the posterior hemisphere of the eyeball. A transverse plane passing through the medial and lateral recti helps to make a further division of the extraconal space into two areas located respectively above and under the muscular pyramid (Fig. 13.1).

Intramuscular Cone

As we have already stated, the intramuscular cone is the space outlined by the four recti. At the level of the eyeball, the sheaths of the four recti are bridged together by the **intermuscular membrane**. Further backward, behind the posterior pole of

CHAPTER 14

Brief Outline of Human Eye Development

Eugenio Bertelli

List of Abbreviations

FGF	Fibroblast Growth Factor	FOXC1	Forkhead box C
PAX	Paired Box	RPC	Retinal Progenitor Cell
SIX	Sine oculis homeobox	SOX	SRY homeobox-like
MAF	Muscoloaponeurotic Fibrosarcoma	M-cones	Medium wavelength cones
Oncogene		L-cones	Long wavelength cones
PITX	Paired-like homeodomain	S-cones	Short wavelength cones

Early Development

By 16 days of gestation, on the dorsum of the developing embryo, the ectoderm has produced a central thickening, the **neural plate** or **neuroectoderm**. Two days later the neural plate shows a sagittal depression, the **neural groove**, encompassed between two parallel **neural folds** (Fig. 14.1). By the end of the third week, the neural folds raise and converge together. In doing so, their tops come into contact and fuse together starting roughly from their midpoint. The fusion of the neural folds, extending caudally and rostrally, transforms the neural groove into the **neural tube** (Fig. 14.1). The extremities of the neural tube, the **neuropores**, eventually close. By 20 days of gestation (2 mm embryo), in proximity of the rostral end of the neural groove, the inner side of the neural folds develops a couple of small lateral grooves (optic sulci) which represent the very first visible event marking the onset of eye development (Fig. 14.2). The sulci, deepening laterally, are then called **optic pits** and they correspond to the optic evaginations that can be seen on the outer surface of the neural tube. When the rostral neuropore closes (24 days of gestation, 3 mm embryo), the optic evaginations expand and form the **optic vesicles**, a pair of hollow outgrowths bulging from the lateral walls of the neural tube almost in contact with the surface ectoderm (Fig. 14.2). The cavity of the optic vesicles remains in continuity with the cavity of the forebrain vesicle. By 27 days of gestation (4 mm embryo) the surface ectoderm opposite to the optic vesicles grows thicker forming the **lens placodes**. The lens placodes and the optic vesicles maintain close relationships, as they are separated only by a very narrow space (Fig. 14.2). It is thought that starting from this moment the development of both the lens placodes and the optic vesicles is coordinated by the secretion of growth factors, particularly **fibroblast growth factors (FGFs)**. The lens placodes invaginate and form the lens vesicles (Fig. 14.3). The formation of the **lens vesicles** is marked on the surface of the embryo by two small depressions, one for each side, referred to as the lens pits. At first, each lens vesicle remains attached to the surface ectoderm through a narrow peduncle, the **lens stalk**, then it detaches (33rd day of gestation). Simultaneously to the formation of the lens vesicles, the optic vesicles grow laterally remaining connected with the forebrain through a constricted portion, the optic stalk. The optic